Strong-Coupling Theory of Charge-Density-Wave Transitions

C. M. Varma and A. L. Simons
Bell Laboratories, Murray Hill, New Jersey 07974

(Received 22 March 1983)

The order-of-magnitude discrepancy between the predictions of the weak-coupling theory of charge-density-wave transitions and the observations is rectified by construction of a microscopic strong-coupling theory. The essential ingredients of the theory are the strong wave-vector dependence of electronically induced anharmonicity and mode-mode coupling which are shown to strongly depress the transition.

PACS numbers: 71.38.+i, 63.10.+q

The Peierls-Fröhlich[1,2] theory of charge-density-wave (CDW) transitions is based on the weak-coupling limit of electron-phonon interactions. It consists of the calculation of the lowest-order phonon self-energy represented in Fig. 1(a); it is mathematically similar to the BCS theory of superconductivity and predicts that the ratio of the jump in the specific heat ΔC at the transition temperature T_c is $\Delta C \simeq 10.2 k_B^2 T_c N(0)$ and that the ratio of the CDW gap Δ at $T=0$ to that at T_c is $2\Delta/k_B T_c \approx 3.52$. Experimental results are typically an order of magnitude at variance with these predictions. For example in $2H$-$TaSe_2$, a mean-field fit to the data gives a jump in the specific heat about 5 times larger[3] and the ratio Δ/T_c is about 8 times larger[4] than the predicted value.

The temperature dependence in the weak-coupling theory arises solely from the Fermi factors in the self-energy shown in Fig. 1(a). More physically, this amounts to the entropy considered in the theory being that of the electrons alone. McMillan[5] observed that the large ratio of Δ/T_c implies that the correlation length in the transition is very small—of the order of a few lattice spacings. This means that phonons over a substantial part of the Brillouin zone are affected (soften) near the transition,[6] and that their contribution to the entropy can be much larger than the electronic entropy. Using the experimental results, McMillan showed that this idea consistently explains the observations. This leaves one, however, with the need for a microscopic strong-coupling theory, which explains why the transition temperature is depressed an order of magnitude from the predictions of the weak-coupling theory even though the gap is a substantial fraction of the Fermi energy (thereby giving the small correlation length), and which explains the strong temperature dependence of phonons near the transition temperature.

The temperature dependence of phonons can arise from Fig. 1(a) (this is negligible), or from mode-mode coupling due to lattice anharmonicity. The interatomic forces in transition metals and compounds can be usefully divided into two contributions: (1) a short-range part arising from the difference in ion-ion and (static) electron-electron interactions and (2) a part from electron-ion scattering. The leading (harmonic) contribution of (2) is Fig. 1(a). The anharmonic contribution from (1) can be estimated; its magnitude in the important region around the critical phonon wave vector can be shown to be small compared to the anharmonic contribution of (2). More significantly, its wave-vector dependence is rather smooth and cannot explain the observed behavior of phonons. The point is that the experiments require that in the region of anomalous phonon dispersion in the high-temperature phase, the phonons be strongly temperature dependent. This means that the anharmonicity must also be strongly wave-vector dependent, so that it provides a stability to such phonons at high temperatures.

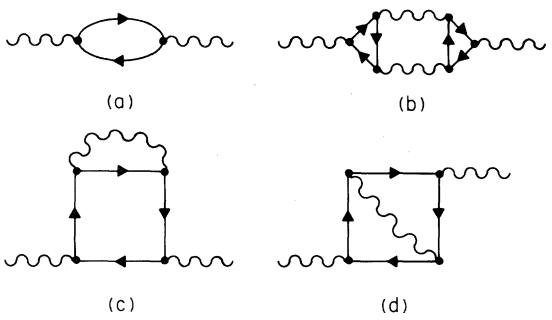

FIG. 1. (a) Irreducible self-energy calculated in the weak-coupling theory of charge-density-wave transitions. The electron-phonon vertices are to be calculated as in Ref. 7. (b) Cubic, and (c), (d) quartic anharmonic self-energy of phonons. The anharmonic vertices arise from multiple electron-phonon scattering as indicated and are strongly wave-vector dependent where the contribution of (a) is large. (d) can be shown to be much smaller than (c) by appeal to Migdal's theorem.

Its effect decreases as temperature decreases. The extra stability must be large enough to drive the transition temperature downwards by an order of magnitude to explain the experiments. We will show here that the Fermi-surface features that lead to anomalous (but nearly temperature-independent) phonon dispersion near specific q vectors due to Fig. 1(a) can also lead to a large wave-vector dependence near such q vectors for the anharmonic interaction. On the basis of this calculation, we construct a strong-coupling theory of CDW transitions.

A method to calculate anomalous phonon dispersion due to Fig. 1(a) has been developed[7] earlier based on the tight-binding representation for electronic structure. A crucial point is that the electron-phonon vertices are strongly momentum dependent and change completely the condition for phonon anomalies from that in the conventional nesting theories.[8] With some approximations, the wave-vector dependence of the electron-phonon matrix elements $g_{kk'}$ is given by[9]

$$g_{kk'} \sim (v_k - v_{k'}), \tag{1}$$

where v_k and $v_{k'}$ are the electronic velocities for initial and final states, respectively, for scattering by a phonon of wave vector $\vec{k}-\vec{k}'$. This method has been used to explain quantitatively the observed phonon anomalies[10] in a wide number of transition metals and compounds. The structural transition[11] at $T=0$ from the bcc to the ω phase in Nb_xZr_{1-x} alloys as a function of x is also explained. Qualitatively, phonon anomalies occur for wave vectors $\vec{q}=\vec{k}-\vec{k}'$ where the difference in electronic velocities $|v_k - v_{k'}|$ is large in the direction $\vec{q}$ and the velocities v_k and $v_{k'}$ are small in a direction transverse to $\vec{q}$. It is easily seen that if the elementary vortex $q_{kk'}$ is large for some $\vec{k}-\vec{k}'$, the vertices in the anharmonic terms in Figs. 1(b) and 1(c) can be even more strongly wave-vector dependent. This will be explicitly seen below.

We have calculated the expression for the anharmonic vertices involved in Figs. 1(b)–1(d). These straightforward but lengthy expressions will not be exhibited here. Suffice it to say that one generates a phonon Hamiltonian

$$H = M\sum_{q\lambda}\omega_{q\lambda}^2 u_{q\lambda}u_{-q\lambda} + \sum V_3(1,2,3)u_1u_2u_3\delta(\vec{q}_1+\vec{q}_2+\vec{q}_3) + \sum V_4(1,2,3,4)u_1u_2u_3u_4\delta(\vec{q}_1+\vec{q}_2+\vec{q}_3+\vec{q}_4), \tag{2}$$

where in the first term we have included the contribution from the short-range force constants as well as the contribution of Fig. 1(a). The second and the third terms are the vertices in Fig. 1(b) and Figs. 1(c) and 1(d), respectively. $u_{q\lambda}$ is the phonon displacement of wave vector $\vec{q}$ and polarization λ; 1 stands for $q_1\lambda_1$, etc.

A free energy based on this Hamiltonian can now be constructed with use of a trial density matrix,

$$\rho_t = \prod_{q\lambda}\exp[-m\Omega_{q\lambda}^2(u_{q\lambda}-\bar{u}_{q\lambda})^2] \tag{3}$$

with

$$F = E - TS, \tag{4}$$

$$E = \mathrm{Tr}(\rho_t H), \tag{5}$$

$$S = k_B(\rho_t \ln\rho_t). \tag{6}$$

$\Omega_{q\lambda}$ and $\bar{u}_{q\lambda}$ are used as variational parameters. This procedure generates the self-consistent harmonic approximation for phonon frequencies[12] and generates an expression for the free-energy,

$$F = \sum_q m\Omega_{q\lambda}^2(T)\bar{u}_{q\lambda}^2 + \sum_q V_4(q,-q,q,-q)\bar{u}_{q\lambda}^4, \tag{7}$$

where for $\bar{u}_{q\lambda}=0$, the phonon frequencies are given by[12]

$$m\Omega_{q\lambda}^2 = m\omega_{q\lambda}^2 + \frac{1}{16}\sum\frac{|V_3(q\lambda,1,2)|^2}{\Omega(1)\Omega(2)}\delta(q+1+2) \times\left(\frac{[1+n(1)+n(2)][\Omega(1)+\Omega(2)]}{\Omega_{q\lambda}^2-[\Omega(1)+\Omega(2)]^2}+\frac{[\Omega(2)-\Omega(1)][n(1)-n(2)]}{\Omega_{q\lambda}^2-[\Omega(1)-\Omega(2)]^2}\right) + \frac{1}{8}\sum V_4(q\lambda,-q\lambda,1,2)\frac{1+2n(1)}{\Omega(1)}\delta(1+2). \tag{8}$$

The last two terms in (8) represent the contributions of Figs. 1(b) and 1(c), respectively, in which the internal phonon lines are self-consistent; thus an infinite number of terms are summed. In Eq. (7)

$\bar{u}_{q\lambda}$ are the static distortions below the transition. Within mode-coupling theory all aspects of the statics and the dynamics of the phase transition for any CDW material can be obtained from Eqs. (7) and (8), provided the coefficients are calculated from the microscopic theory described.

The microscopic theory requires the knowledge of the electronic structure for any given material and of the variation of tight-binding integrals with distance. To establish the physical points we have performed calculations with a simplified band structure described by Inglesfield,[13] in which only nearest-neighbor Ta bonds are considered, which is a fair representation of the band structure of $1T$-TaS_2 near the Fermi surface. $1T$-TaS_2 has a CDW transition at wave vector $q \simeq 0.57$, with longitudinal polarization, along the ΓM direction at $T \approx 350$ K. The contribution of Fig. 1(a) to the phonon frequency at $T = 0$ (already calculated by Inglesfield) is shown in Fig. 2, at two temperatures 0 and 10^3 K. An anomaly at the right wave vector is predicted, but as discussed earlier the temperature dependence is negligible. (It will be soon obvious that with this contribution alone the transition temperature would be predicted to be a few thousand degrees!) Also shown in Fig. 2 is one of the fourth-order anharmonic coefficients (the largest). They peak sharply near the critical wave vectors as discussed. Their contribution to stabilize the phonon frequencies will be considerably smoother, since integrals over the zone and many different anharmonic coefficients are involved.

In Fig. 3 the longitudinal phonon frequencies along the ΓM direction in the high-temperature phase are shown for various temperatures with calculations using Eq. (8). Just as in previous theory the short-range harmonic force constants are parametrized (two parameters for nearest-neighbor forces only) to fix the sound velocities. No adjustable parameter enters in the calculation of the temperature dependence or in calculation of Fig. 1(a). The strong stabilizing effect of the anharmonic phonons in the anomalous zone is evident. On the basis of the temperature dependence of the phonons around the critical wave vector, the specific heat near the transition can be calculated. Just as in any mode-coupling theory the prediction is $(2\pi\xi_0)^{-3}[(T - T_c)/T_c]^{-1/2}$ per unit cell in three dimensions, where ξ_0 is the correlation length obtainable from the calculated phonon dispersion. If we assume that the correlation length in the direction transverse to the hexagonal

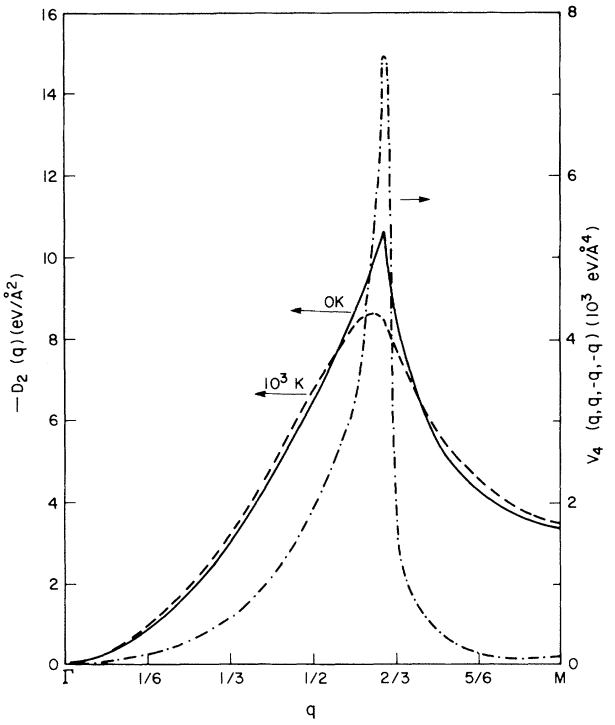

FIG. 2. Left scale: The contribution of Fig. 1(a) to the self-energy of longitudinal phonons along ΓM at 0 and 10^3 K. Right scale: One of the anharmonic coefficients with all q along ΓM and all polarization longitudinal. Calculations have used a model band structure for $1T$-TaS_2.

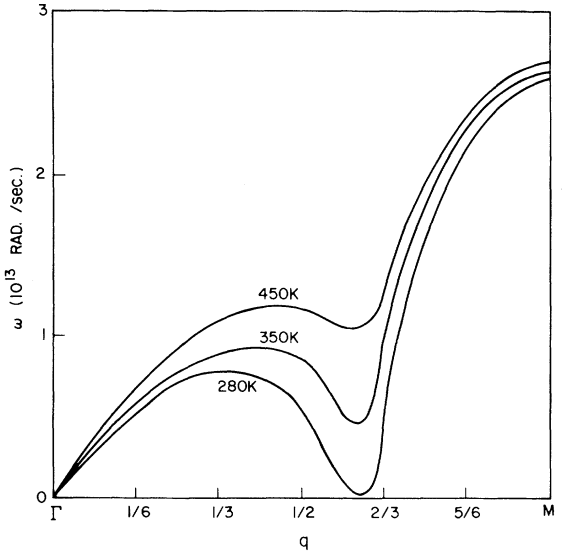

FIG. 3. Longitudinal phonon frequencies in the ΓM direction for various temperatures, calculated as described in the text.

planes is similar to that in the plane, we get an upper limit to correlation length ξ_0, from our calculated phonon dispersion near T_c, given by $\pi\xi_0 \lesssim 20$ Å. Experiments on high-quality crystals of $2H$-$TaSe_2$ have been quantitatively analyzed to give[3] $C(T) \approx (2\pi\xi_0)^{-3}[(T-T_c)/T_c]^{-0.45 \pm 0.035}$ with $\pi\xi_0 \approx 14$ Å. The agreement of the theoretical exponent with the experimental value is not significant; we cannot claim to have a correct theory in the critical regime. What is significant is that we obtain the correct magnitude of the correlation length from the microscopic strong-coupling theory. From this correlation length, we estimate $2\Delta/T_c \gtrsim 23$ compared to the experimental value for $2H$-$TaSe_2$ of ~28 and a mean-field value of 3.52. It may be argued that our calculations are for $1T$-TaS_2 while we are comparing with results for $2H$-$TaSe_2$. The point is that the strong-coupling effects are similar in magnitude for all CDW transitions which have been carefully measured.[14] For $1T$-TaS_2, where the band structure is simple enough to perform the first calculations with the theory presented here to establish the basic physical points, only room-temperature neutron scattering results are available.[15] Comparison of these results with the neutron scattering results from $2H$-$TaSe_2$ (Ref. 6) at the same normalized temperature (normalized with respect to T_c) yields the result that the two materials have nearly the same correlation length ξ_0.

In summary, we have constructed a microscopic theory for the statics and dynamics of strong-coupling charge-density-wave transitions. The theory entails a calculation of the wave-vector dependence of anharmonicity and the temperature dependence of phonons. Electronically induced anharmonicity and mode-mode coupling are shown to lead to a large depression in transition temperatures, thus explaining the short correlation length and the consequent large observed values of Δ/T_c and the specific heat near the transition.

[1]R. E. Peierls, *Quantum Theory of Solids* (Clarendon, Oxford, 1955).

[2]A. Fröhlich, Proc. Roy. Soc. London, Ser. A 223, 296 (1954).

[3]R. A. Craven and S. F. Meyer, Phys. Rev. B 16, 4583 (1977).

[4]A. S. Barker, Jr., J. A. Ditzenberg, and F. J. DiSalvo, Phys. Rev. B 12, 2049 (1975).

[5]W. L. McMillan, Phys. Rev. B 16, 643 (1977).

[6]D. E. Moncton, J. D. Axe, and F. J. DeSalvo, Phys. Rev. Lett. 34, 734 (1975), and Phys. Rev. B 16, 80 (1977).

[7]C. M. Varma and W. Weber, Phys. Rev. Lett. 39, 1094 (1977), and Phys. Rev. B 19, 6142 (1979).

[8]A. W. Overhauser, Phys. Rev. 167, 691 (1968); S. K. Chan and V. Heine, J. Phys. F 3, 795 (1973).

[9]C. M. Varma, E. I. Blount, P. Vashista, and W. Weber, Phys. Rev. 19, 6130 (1979). This result was derived in a simple model earlier by S. Barisic, J. Labbe, and J. Friedel, Phys. Rev. Lett. 25, 919 (1970).

[10]For a review, see W. Weber, in *Superconductivity in d- and f-Band Metals*, edited by H. Suhl and M. B. Maple (Academic, New York, 1980).

[11]A. L. Simons and C. M. Varma, Solid State Commun. 35, 317 (1980).

[12]See, for example, articles by H. Horner and by W. Götze, in *Lattice Dynamics*, edited by A. A. Maradudin and G. K. Horton (North-Holland, Amsterdam, 1975).

[13]J. E. Inglesfield, J. Phys. C 13, 17 (1980).

[14]Thus for instance $\Delta C/T_c$ for $2H$-$TaSe_2$ (Ref. 3), $2H$-TaS_2 (Ref. 3), and $2H$-$NbSe_2$ [J. H. Harper, T. H. Geballe, and F. J. DiSalvo, Phys. Lett. 54A, 27 (1975)] are 3.3×10^{-2}, 3.6×10^{-2}, and 4×10^{-2} J/mole K^2, respectively.

[15]K. R. A. Ziebeck *et al.*, J. Phys. F 7, 1139 (1977).